

Thermodynamics of Catalytic Formation of Dimethyl Ether from Methanol in Acidic Zeolites

Marek Hytha,^[b, c] Ivan Štich,^{*[a]} Julian D. Gale,^[d] Kiyoyuki Terakura,^[e, f] and Michael C. Payne^[g]

Abstract: We present a theoretical study of the formation of the first intermediate, dimethyl ether, in the methanol to gasoline conversion within the framework of an ab initio molecular dynamics approach. The study is performed under conditions that closely resemble the reaction conditions in the zeolite catalyst including the full topology of the framework. The use of the method of thermodynamic integration allows us to extract the free-energy

profile along the reaction coordinate. We find that the entropic contribution qualitatively alters the free-energy profile relative to the total energy profile. Different transition states are found from the internal and free energy profiles. The entropy contribution varies

significantly along the reaction coordinate and is responsible for stabilizing the products and for lowering the energy barrier. The hugely inhomogeneous variation of the entropy can be understood in terms of elementary processes that take place during the chemical reaction. Our simulations provide new insights into the complex nature of this chemical reaction.

Keywords: catalysts • density functional calculations • thermodynamics • zeolites

Introduction

One of the most studied industrial applications of zeolites in current commercial production is the methanol-to-gasoline (MTG) process^[1] for catalytic conversion of methanol to

hydrocarbons. There is a large volume of experimental evidence that methanol, when catalyzed by an acidic zeolite, is first dehydrated to dimethyl ether (DME) which is then, in combination with methanol, converted to hydrocarbons up to C₁₀. The industrial process is catalyzed by ZSM-5 and proceeds at high methanol loadings of $\approx 5-6$ methanol molecules per acidic hydroxyl group^[2] at a temperature of 700 K. The whole process involves a number of steps of increasing complexity: i) the initial methanol adsorption, ii) activation of the adsorbed species, iii) dehydration to DME, and iv) formation of the C–C bond. It has, however, proved difficult to understand the role of the zeolite catalyst in the first three stages of the MTG process, because experiments, typically IR spectroscopy, do not provide a sufficiently complete and detailed atomistic picture of the process, since they rely on interpretation in terms of an existing model. Recently, ab initio theoretical studies have started to shed light on these processes.^[3–6] The first two points have been extensively studied in our previous papers.^[7, 8] The focus of the present paper is the formation of DME in the zeolite under reaction conditions.

The initial methanol adsorption has been the subject of numerous studies.^[6–11] A consensus has emerged that as soon as the methanol loading reaches two molecules per acid site, methanol is chemisorbed as a methoxonium cation (CH₃–OH₂⁺). A more complete statistical sampling of the underlying potential energy surface was required to elucidate the activation of the adsorbed species.^[7, 8] Solvation of the methoxonium ion in the methanol solvent has been found to further soften the methoxonium C–O bond.^[8] However,

[a] Prof. I. Štich

CCMS, Department of Physics
Slovak Technical University (FEI STU)
Ilkovičova 3, 812 19, Bratislava (Slovakia)
Fax: (+421) 7-654-11-483
E-mail: stich@elf.stuba.sk

[b] Dr. M. Hytha

National Center for High Performance Computing
P. O. Box 19-136, Hsinchu (Taiwan)

[c] Dr. M. Hytha

Institute of Physics of the Czech Academy of Sciences
Cukrovarnicka 10, 16253 Prague 6 (Czech Republic)

[d] Dr. J. D. Gale

Department of Chemistry
Imperial College of Science, Technology and Medicine
South Kensington, London SW7 2AY (UK)

[e] Prof. K. Terakura

JRCAT, Angstrom Technology Partnership (ATP)
1-1-4 Higashi, Tsukuba, Ibaraki 305-0046
Japan National Institute for Advanced Interdisciplinary Research
1-1-4 Higashi, Ibaraki 305-8562 (Japan)

[f] Prof. K. Terakura

CREST, Japan Science and Technology Corporation
Kawaguchi, Saitama 332 (Japan)

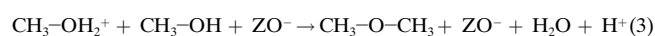
[g] Prof. M. C. Payne

Cavendish Laboratory, Madingley Road
Cambridge CB3 0HE (UK)

activation was only found to occur if the mobility of the methoxonium ion, promoted by certain zeolite frameworks or by high temperature, prevents it from forming hydrogen bonds with the zeolite channel and with the other methanol molecules.^[8] Such strongly activated methoxonium complexes are expected to form DME easily. Experiments suggest a dramatic increase in DME formation in a narrow temperature interval around 500 K.^[12] Different mechanisms have been proposed for the formation of DME. Bandiera and Naccache have proposed the existence of two surface species $\text{CH}_3\text{-OH}_2^+$ and CH_3O^- , forming at the Brønsted acid and its adjacent Lewis basic sites,^[13] which can condense to produce DME and water. In the “indirect” pathway^[14, 15] the DME formation proceeds via a surface methoxy intermediate [Eq. (1)], which subsequently reacts with another methanol molecule to form DME [Eq. (2)].



Here Z stands for the zeolite framework. We assume here that the methanol is chemisorbed at an acid site as the protonated complex, since this is expected to be more susceptible to nucleophilic attack. Alternatively, in the “direct” pathway^[5, 6] [Eq. (3)], both methanol molecules react with each other inside the zeolite environment which acts merely as a solvent.



In above reaction we have not specified the final destiny of the zeolitic proton, as our simulations performed under conditions which emulate those of the true reaction suggest (See Results and Discussion) that this proton may be mobile and need not necessarily permanently bind to the Brønsted site. Additionally there are competing pathways in which methanol reacts to form a carbon–carbon bond, for instance yielding ethanol and ethene by further dehydration. However, the activation energy for this process has been shown to be much higher than that for formation of dimethyl ether.^[3]

Unfortunately, very little is known about the energetics of DME formation experimentally. Bandiera and Naccache have estimated that the true activation energy for the condensation of methanol is approximately 80 kJ mol^{-1} ($\approx 0.83 \text{ eV}$) for H-Mordenite with a low aluminum content.^[3] However, the barrier height will be sensitive to methanol coverage, as well as to the particular zeolite and composition studied. On the other hand, several theoretical studies of the dehydration process exist. Blaskowski and van Santen^[5] calculated the energetics of both direct and indirect processes using a small cluster model for the zeolite and density functional theory (DFT). Shah et al.^[6] investigated both pathways for DME formation in chabazite from two methanol molecules within the framework of DFT. Both studies conclude that the direct mechanism is preferred over the indirect one. Very recently, Sandré et al.^[16] determined the transition-state structure and energy for the direct pathway for the system investigated in reference [6] (two methanol molecules in chabazite) and

determined the total energy profile along the reaction coordinate. The total energy barrier for this process was found to be $\sim 0.7 \text{ eV}$ starting from a configuration in which the two methanol/methoxonium molecules are oriented such that they can react. This configuration is not necessarily the lowest energy configuration. Hence, the “reorientation” energy needed to reorient the methyl and hydroxyl groups of the two reacting methanol molecules so that they can react along the $\text{S}_{\text{N}}2$ pathway should be added to this calculated energy barrier. In the cluster model given in reference [5] the reorientation energy is found to be $\sim 0.5 \text{ eV}$, which is slightly lower than estimates from periodic calculations of $\sim 0.6 \text{ eV}$.^[6]

All these previous studies were based on transition-state theory^[17] with the free energy profile approximated either by the internal energy or with the estimation of the entropy from the internal energy within the harmonic approximation. However, as we show below, the maxima in the free and total energy may *not* coincide; this makes such an approach *invalid* for the present reaction. Our previous work has shown^[7, 8] that it is important to sample configuration space more widely than just the lowest internal energy path as the energy surface is very shallow with multiple minima about the reaction coordinate. A consequence of this is a huge and non-uniform entropy contribution that cannot be treated correctly within the harmonic approximation. Such a behavior is symptomatic of systems with complicated high-dimensional transition states^[18] whose position may not be known a priori. Our present calculations are based on thermodynamic integration techniques^[19–21] within ab initio molecular dynamics (MD).

The paper presents the most complex and comprehensive simulation performed to date of formation of the first intermediate in the MTG process. The simulations reveal several new features and pitfalls that would remain hidden in a more simplified approach. In the next section we introduce our model and simulation techniques. Our main results and discussion are presented in the Results and Discussion.

Computational Methods

The model: The model considered in our study has been carefully chosen. The commercial catalyst ZSM-5 has a unit cell with ≈ 300 atoms; this is too large for the present simulations to be practical.^[22] For that reason the simulations were performed in ferrierite,^[23] which has a much smaller unit cell, with only 54 atoms, but a structure very similar to that of ZSM-5 (Figure 1). The ferrierite structure is the closest mimic to the ZSM-5 structure we were able to find. In particular, it has two channels, a ten-ring channel similar to the straight channel in ZSM-5 and another straight channel with an eight-ring aperture, perpendicular to the ten-ring channel. Only one Brønsted acid site was considered, corresponding to a Si/Al ratio of 18. Given the dearth of experimental data and the computational cost of the present simulations no other Si/Al ratio was attempted. The location of the Brønsted acid site (Al on T4 and the proton initially on O6) and the consequences of this choice have been discussed elsewhere.^[8] The reaction conditions have been simulated by loading four methanol molecules into the eight-ring channel and associated intersection regions of ferrierite (Figure 2). The system was prepared so that two methanol molecules (#1 and #2 in Figure 2) can react along the $\text{S}_{\text{N}}2$ pathway. The temperature in the simulation was taken to be 700 K. This system was shown to form strongly activated methoxonium species.^[8] The activated species are expected to be susceptible to a nucleophilic attack by another methanol molecule to give rise to reaction given in Equation (3). The ability of this system to exhibit activation makes this system a strong contender for the direct reaction pathway.

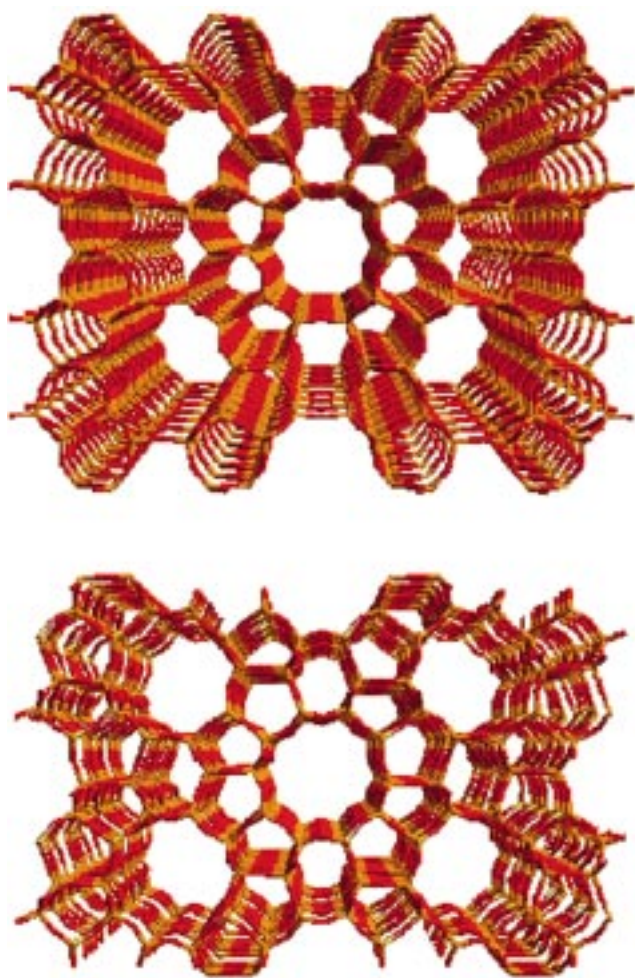


Figure 1. Perspective view of the structures of ferrierite (upper panel) and ZSM-5 (lower panel) along the (straight) ten-ring channel.

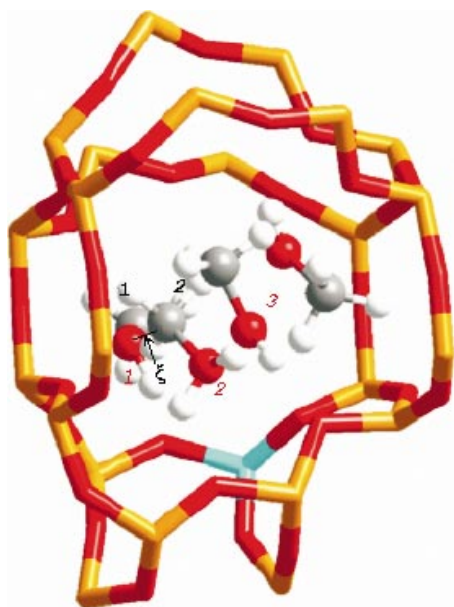


Figure 2. The model for DME formation. Four methanol molecules are loaded in the eight-ring channel. The black numbers label the carbon atoms and the red numbers the oxygen atoms in the methanol molecules. Molecule #2 underwent spontaneous protonation and forms a methoxonium cation. The holonomic constraint ξ is applied to oxygen #1 and carbon #2. The aluminum defect is shown in blue.

Ab initio MD simulations: Ab initio MD simulations^[24] have been performed for the formation of DME. All technical details of our simulations are as described in reference [8]. It suffices to say that simulations were run in the (N,V,T) ensemble by using DFT in its plane-wave pseudopotential formulation. Hence, periodic boundary conditions allow us to consider the full zeolite topology. Gradient corrected functionals were required for an accurate description of the DME formation and we used the PW'91^[25] variant of the GGA approximation to the DFT. We used norm-conserving pseudopotentials to represent the core electrons and the wave functions of the valence electrons were expanded in plane waves at the Γ point of the supercell with a cut-off of 40 Ryd. The accuracy of the DFT in the present GGA approximation was extensively tested previously.^[6, 8, 10] It was found that it yields excellent equilibrium methanol geometries, harmonic frequencies, proton affinities, quartz formation energies, etc. The main DFT uncertainty remains in the region around the transition state at which DFT is usually less accurate than around the reactant/product wells. We expect the huge non-uniform entropic corrections computed beyond the harmonic approximation to be the major ingredient missing in all previous DFT calculations that make use of identical or similar GGA energy functionals.

Thermodynamic integration: Thermodynamic integration was performed by using the so-called “Blue Moon” ensemble^[19–21] to overcome the large reaction barrier and to evaluate the entropic contribution along the reaction coordinate. This is a well-known approach; however, it has not been applied very often to complex chemical systems.^[26] We have performed constrained MD by adding a holonomic constraint to the Lagrangean generating the MD given in Equation (4).

$$\mathcal{L} = \sum_{i=1}^N \frac{1}{2} M_i \dot{\vec{R}}_i^2 - U(\{\vec{R}_i\}) + \lambda_\xi [\xi\{\vec{R}_i\} - \xi_0] \quad (4)$$

The first term on the right-hand side of Equation (4) is the kinetic energy of the N ions, $U(\{\vec{R}_i\})$ is the many-body potential energy, equal to the Kohn–Sham energy, and λ_ξ is the Lagrange multiplier for the reaction coordinate $\xi\{\vec{R}_i\}$. In the present case of DME formation by the direct path, the reaction coordinate is the distance $|\vec{R}_{\text{CH}_3} - \vec{R}_{\text{OH}}|$ between the methyl group of the methoxonium ion and the hydroxyl group of one of the other methanols (c.f. Figure 2) and ξ_0 is the externally fixed value of that distance. The constrained dynamics run was started from a well-equilibrated, unconstrained configuration taken from the study described in reference [8]. The constrained dynamics was run for ten values of the constraining distance ξ_0 ; the length of each run was ≈ 2 ps after equilibration. The Helmholtz free-energy profile was computed by using Equation (5) in which R refers to

$$\Delta F(\xi, T) = \int_R^P \langle \lambda_\xi \rangle_{\xi_0, T} d\xi_0 \quad (5)$$

reactants and P to products and the thermodynamic averaging $\langle \dots \rangle_{\xi_0, T}$ is performed by averaging over the MD trajectories. We note that Equation (5) is correct only for a constraint consisting only of a distance $\xi = |\vec{R}_i - \vec{R}_j|$. The formulae for a more general case can be found in reference [21].

One potential problem with the application of Equation (5) to chemical reaction in which one chemical bond is broken and a new one is formed with a simple control by one distance constraint ξ is that all degrees of freedom, except for that constrained by ξ , must be in equilibrium along the reaction coordinate to give the correct free energy. For example, up to the transition state, reaction $A + B-C \rightarrow A-B + C$ can be controlled by constraining the distance between A and B with all other degrees of freedom in equilibrium and with the process being reversible. However, past the transition state it may not be possible to control the distance between B and C by the constraint ξ corresponding to the distance between A and B . Hence, in such a case the distance between A and B no longer corresponds to the reaction coordinate and the free energy cannot be obtained from Equation (5). In general, all breaking and forming chemical bonds whose reaction barriers are large enough relative to the thermal energies should be controlled by an additional constraint. An elegant solution to this problem, the so-called transition-path ensemble, was proposed recently by Chandler et al.^[18] In this approach, neither the transition state nor the potentially very complicated transition path from the reactant to the product well need be explicitly known or specified. The only technical problem with this promising approach is its additional

computational cost. To our knowledge, the method has not yet been applied to a chemical reaction in an ab initio fashion. Hence, our approach goes midway between the customary approximations based on the transition-state theory and one-dimensional internal energy surface, and a transition path ensemble approach. Consequences of our approach for reliability of our results will be addressed in the next section.

Results and Discussion

The Lagrange multipliers along the reaction coordinate, which ensure that the distance between the C atom on the methoxonium cation and the O atom on the other methanol molecule (Figure 2) remains fixed, are shown in Figure 3.

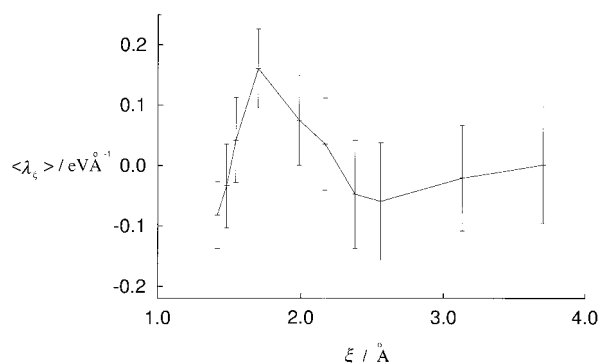


Figure 3. Variation (in eV \AA^{-1}) along the reaction coordinate ξ of the Lagrange multipliers $\langle \lambda_\xi \rangle$.

These Lagrange multipliers are required to compute the free energy profile from Equation (5). The computed free energy profile, the total energy [Eq. (6)], and the entropy profile [Eq. (7)] are shown in Figure 4.

$$E_{\text{tot}}(\xi) = \sum_{I=1}^N \frac{1}{2} M_I \dot{R}_I^2 + U(\{\vec{R}_I\}) \quad (6)$$

$$TS(\xi) = E_{\text{tot}}(\xi) - F(\xi) \quad (7)$$

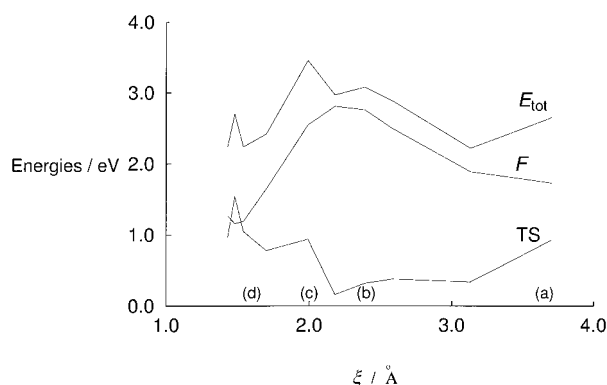


Figure 4. Variation along the reaction coordinate ξ of the free-energy profile $\Delta F(T=700 \text{ K})$; total-energy profile $\Delta E_{\text{tot}}(T=700 \text{ K})$, and the entropy contribution TS . The zero of the vertical scale is arbitrary. (a)–(d) label the configurations shown in Figure 5.

Note that, unlike $E_{\text{tot}}(\xi)$, the zeroes of the $F(\xi)$ and $S(\xi)$ profiles are arbitrarily defined, and we only determine the profiles relative to the thermodynamic state of the reactants.

To give a better insight into the reaction process, we show in Figure 5 characteristic configurations sampled from the MD trajectories of the reacting molecules in a) the reactant well,

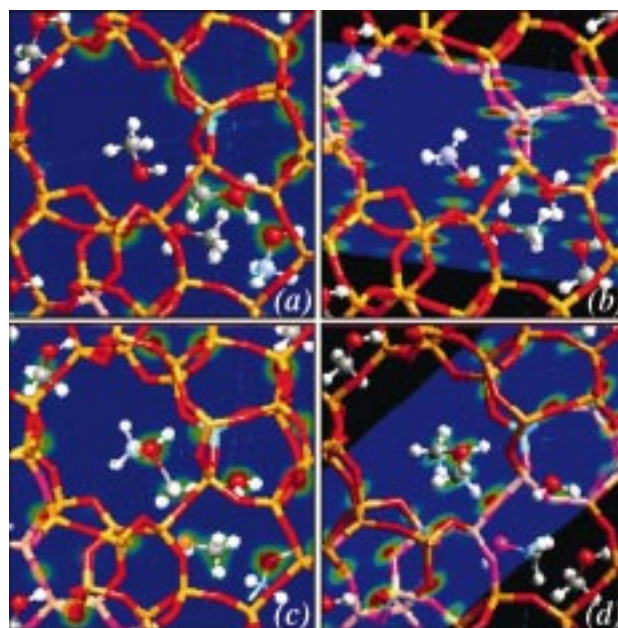


Figure 5. Ball and stick models with superimposed valence electronic charge densities for points (a)–(d) along reaction coordinate defined in Figure 4. The electronic charge density is shown on a plane defined by the oxygen #1, carbon #2, and the Al defect (Figure 2).

b) and c) near the transition state, and d) in the product well. Figure 5a shows a configuration with the constraint ξ_0 which corresponds to the value of the Lagrange multiplier $\langle \lambda_\xi \rangle = 0$. In this configuration the zeolitic proton, which originally formed part of one methoxonium cation $\text{CH}_3\text{-OH}_2^+$, is shared by two methanol molecules and executes a motion in a double-well type of potential surface by hopping between the two methanol molecules. The configuration in Figure 5b corresponds to the transition state in the free-energy profile, at which the water starts to dissociate from the methoxonium cation. In Figure 5c the water molecule is completely dissociated and a new chemical bond is forming between the methyl group of the methoxonium cation and one of the methanol molecules. This configuration corresponds to the transition state from the total energy curve. Figure 5d shows the configuration corresponding to the minimum of the free energy profile, at which protonated DME was formed. Only a further compression of the bond by the applied constraint ($\xi_0 \approx 1.42 \text{ \AA}$) led to deprotonation of DME. This proton then became rather mobile on our MD scale. It moved away from the DME to form a hydroxonium cation. As a result the total energy E_{tot} in Figure 4 started to decrease again; this suggests that this configuration is energetically more stable than the configuration with protonated DME. Additional understanding of the complexities of this reaction, including the mobility of the zeolitic proton, reactants, and products can be obtained from a computer graphics animation.^[27]

Given the fact that a very simple form of the reaction coordinate ξ was assumed and a single constraint applied to

control the reaction, it is important to assess the correctness of this choice. Two processes take place as the system climbs the reaction barrier. The applied constraint forces the formation of a chemical bond between the oxygen in the methanol #1 and the carbon atom on the methoxonium ion #2 (Figure 2). During this process [Eq. (3)] methoxonium is dehydrated which breaks the $\text{H}_3\text{C}-\text{OH}_2^+$ bond. However, these two processes do *not* take place simultaneously. We find that the water molecule from the $\text{CH}_3-\text{OH}_2^+$ complex dissociates near $\xi \approx 2.38 \text{ \AA}$, before the other (C–O) bond is formed around $\xi \approx 2.0 \text{ \AA}$. The global maximum/saddle point corresponds to the transition state from the $E_{\text{tot}}(\xi)$ profile. Hence, there is no competition between breaking and forming chemical bonds. In particular, for $\xi < 2.38 \text{ \AA}$ the dissociated water does not take any active part in the DME formation and comes to equilibrium by optimizing the alignment of its dipole moment. If this were not the case at least two constraints would be required to follow the correct reaction path. In order to check the reversibility of the process tests have been made around the maximum/saddle point. In further checks we were able to locate another (metastable) configuration for $\xi_0 = 2.16 \text{ \AA}$ with water still bonded in the $\text{CH}_3-\text{OH}_2^+$ complex. However, E_{tot} in this arrangement was $\approx 0.4 \text{ eV}$ higher than for the configuration with the water molecule already dissociated. On the other hand, configurations with dissociated water for $\xi_0 > 2.38 \text{ \AA}$ were unstable and spontaneously relaxed to the arrangement corresponding to the $\text{CH}_3-\text{OH}_2^+$ complex. Hence, the thermodynamically stable reaction path is the one given in Figure 4 and our choice of the reaction coordinate ξ is meaningful.

From Figure 4 we see that the total- and free-energy profiles along the reaction coordinate differ appreciably even at a qualitative level. In particular, the entropic contribution to the reaction barrier is of the same order as the internal energy contribution and, hence, any conclusion reached without explicitly including the entropy will be incorrect. This finding may not appear surprising at $T = 700 \text{ K}$. However, to the best of our knowledge, the huge non-uniform entropic corrections have never been properly treated in theoretical modeling of the MTG process to date.

The main findings from Figure 4 can be summarized as follows:

- 1) The transition states deduced from the $F(\xi)$ and $E_{\text{tot}}(\xi)$ profiles do not coincide, hence different triggering processes for the reaction are deduced from $F(\xi)$ and $E_{\text{tot}}(\xi)$.
- 2) The total-energy curve $E_{\text{tot}}(\xi)$ shows a local minimum close to the transition state.
- 3) The entropy profile $S(\xi)$ varies considerably along the reaction coordinate.
- 4) The minima of $F(\xi)$ and $E_{\text{tot}}(\xi)$ curves do not coincide, hence they yield different reactant and product equilibrium geometries.
- 5) In contrast with the result for total energy, the minimum on the product side of the free-energy curve is significantly ($\approx 0.5 \text{ eV}$) lower than on the reactant side, and, therefore, is entropy stabilized.

- 6) The free energy barrier is entropically lowered relative to the internal energy barrier.

We now discuss these features more in detail. The internal-energy curve $E_{\text{tot}}(\xi)$ exhibits two activated processes: dissociation of water from the methoxonium cation around $\xi \approx 2.38 \text{ \AA}$ and reaction of the methyl group with the other methanol around $\xi = 2 \text{ \AA}$, separated by a minimum. The latter process corresponds to the transition state from $E_{\text{tot}}(\xi)$. On the other hand, the transition state from the $F(\xi)$ profile corresponds roughly to the former process of dissociation of water from the methoxonium cation. This clearly shows that the customary assumption of the dominance of the internal energy is not valid and that a more complex MD sampling of the internal energy surface is required.

The sampling of the flat anharmonic multi-minima internal-energy surface leads to the huge and non-uniform variation of the entropic profile $S(\xi)$. As the entropy associated with the zeolite catalyst is approximately constant the complicated $S(\xi)$ profile can be understood in terms of elementary molecular processes as follows. Up to the transition state, the entropy decreases as a function of ξ . This is caused by two different processes that lead to reduced mobility of the reacting methanol molecules. First, the two molecules are “glued” together by sharing the zeolitic proton (Figure 5a). This proton moves between two methanol molecules (#2 and #3 in Figure 2);^[8] this results in a very large root mean square (rms) fluctuation of the O–H distance when ξ is around 3.17 \AA (Figure 6). A consequence of this proton transfer is

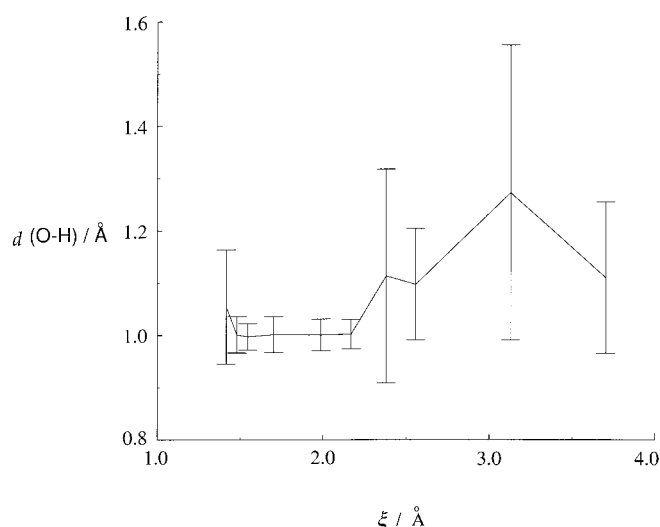


Figure 6. Variation along the reaction coordinate of the O–H bond length of the proton on the methoxonium cation, which is shared with a nearby methanol molecule.

that these two methanol molecules are effectively glued together by this proton. This results in a reduction of their mobility and, hence, a lowering of the entropy $S(\xi)$. A similar process can be seen to occur in Figure 5b, in which the methyl group is now shared between the dissociating water and the reacting methanol and, hence, glues these groups together. Beyond the transition state a new molecule is formed, which is

initially characterized by one ($\text{CH}_3\text{OH}^+-\text{CH}_3$) very loose chemical bond. Such behavior is clearly visible in Figure 7, which shows the $\text{CH}_3-\text{OH}_2^+$ bond length with its rms fluctuations along the reaction coordinate. In the region $\xi \approx 2 \text{ \AA}$ this loose bond is responsible for the steep increase in the entropy. As can be deduced from the behavior

Conclusion

We have presented the first ab initio MD simulation of dehydration of methanol to DME catalyzed by an acidic zeolite under reaction conditions. The use of the method of thermodynamic integration allowed us to perform a simulation of this chemical reaction on MD observation timescales and to evaluate the entropy profile along the reaction coordinate. The central result of this paper is that the condensation reaction of methanol at reaction temperature by the “direct” pathway is a process that exhibits strong qualitative and quantitative differences between the total-internal- and free-energy profiles. Qualitatively, the total-energy profile locates a different transition state and the profile itself has a completely different structure compared with the free-energy profile. In particular, the transition state in the E_{tot} profile corresponds to a state at which the H_3C^+ -complex starts reacting with the other methanol molecule to form DME, whereas the transition state found from the free-energy profile corresponds to a state at which water dissociates from the $\text{CH}_3-\text{OH}_2^+$ complex. Quantitatively, the hugely inhomogeneous entropy profile is responsible for stabilizing the products by $\approx 0.5 \text{ eV}$ and for lowering of the free-energy barrier relative to the total energy barrier. Evidently, we have a system in which the assumptions commonly made when approximating the free-energy profile by the $T=0$ total-energy profile would lead to incorrect theoretical predictions.

The approach adopted here combines the well-known technique of thermodynamic integration, required to extract the entropy contribution beyond the harmonic approximation, with ab initio MD, needed to sufficiently accurately describe the breaking/forming of chemical bonds in the chemical reaction. The main complication with this approach is the rather high computational cost. However, the class of systems and processes with entropically controlled behavior and/or with complicated multidimensional, difficult to locate, transition states is large, and the techniques of thermodynamic integration^[21] and transition-path ensemble^[18] will play an increasingly important role in a realistic study of chemical reactions.

We believe that the main uncertainty of our calculations is in studying the dehydration process in the eight-ring channel of ferrierite. Some of the processes we observed might be altered if the reaction were studied in a channel with a different aperture or in a different zeolite framework. Unfortunately, the available experimental results^[13] taken under different conditions and in different frameworks make it difficult to make a direct comparison. Nevertheless our simulations have shown new features and behavior in this reaction which could be uncovered only by present techniques. More simulations of this reaction under different conditions, such as in different zeolite catalyst, different channels, and under different Si/Al ratio can be performed when more experimental data become available. Currently, simulations similar to those presented here are underway for the reaction leading to the formation of the first C–C bonds under reaction conditions.

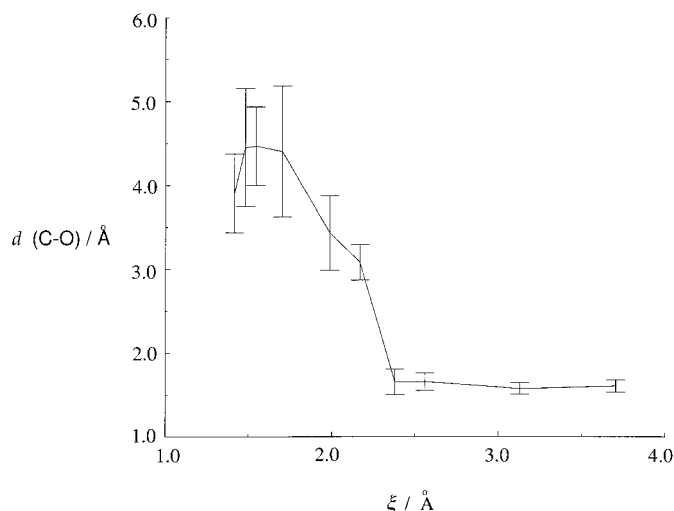


Figure 7. Variation along the reaction coordinate of the $\text{CH}_3-\text{OH}_2^+$ bond length (carbon and oxygen atoms on molecule #2 in Figure 2).

of entropy around the minimum of $F(\xi)$ the protonated DME is characterized by an increase in the number of possible configurations. The steep decrease in entropy for the smallest value of ξ is caused by deprotonation of DME which makes the product stiffer. The variation of the $S(\xi)$ profile explains also the other features above.

In addition to locating the pathway for reaction to form dimethyl ether, there is another notable observation made during the constrained dynamics. For several different constraint values it is found that the oxygen of one of the methanol molecules is able to approach a silicon of the framework to within 1.8 \AA , which is within the upper bound of the vibrational fluctuations of the framework oxygens. This means that for the order of a few vibrational periods silicon becomes approximately five coordinate. While these states are clearly unstable and transitory in nature, it indicates that the dynamical flexibility of the zeolite is sufficient to fleetingly accommodate higher silicon coordination. This observation was not confined to one particular methanol or silicon atom; it occurred for several different cases along the reaction pathway. Previous unconstrained dynamical runs^[7,8] had not highlighted this feature. This could be either because the close approach is only feasible as the system passes through a reactive configuration, or alternatively because of the much longer total sampling time for the constrained dynamics making the observation of such events more probable. While “floating bonds” associated with five-fold coordinated Si atoms have long been considered a viable possibility in amorphous Si networks,^[28] their existence in zeolite frameworks has not previously been proposed.

Acknowledgements

I.S. and K.T. acknowledge Dr. M. Sprik and Dr. M. Boero for valuable comments on constrained dynamics. The calculations reported here were performed on the JRCAT supercomputer system. This work was partly supported by the New Energy and Industrial Technology Development Organization (NEDO). I.S. thanks ATP for support in this research. J.D.G. acknowledges the Royal Society for a University Research Fellowship. M.C.P. and K.T. thank the British Council for a Collaborative Research Project Award.

- [1] S. L. Meisel, J. P. McCulloch, C. H. Lechthaler, P. B. Weisz, *Chem. Technol.* **1976**, 6, 86.
- [2] G. Mirth, J. A. Lercher, M. W. Anderson, J. Klinowski, *J. Chem. Soc. Faraday Trans.* **1990**, 86, 3039.
- [3] S. R. Blazzkowski, R. A. van Santen, *J. Am. Chem. Soc.* **1997**, 119, 5020.
- [4] S. R. Blazzkowski, R. A. van Santen, *J. Phys. Chem.* **1995**, 99, 11728.
- [5] S. R. Blazzkowski, R. A. van Santen, *J. Am. Chem. Soc.* **1996**, 118, 5152.
- [6] R. Shah, J. D. Gale, M. C. Payne, *J. Phys. Chem. B* **1997**, 101, 4787.
- [7] I. Štich, J. D. Gale, K. Terakura, M. C. Payne, *Chem. Phys. Lett.* **1998**, 283, 402.
- [8] I. Štich, J. D. Gale, K. Terakura, M. C. Payne, *J. Am. Chem. Soc.* **1999**, 121, 3292.
- [9] F. Haase, J. Sauer, *J. Phys. Chem.* **1994**, 98, 3083; F. Haase, J. Sauer, *J. Am. Chem. Soc.* **1995**, 117, 3780; F. Haase, J. Sauer, J. Hutter, *Chem. Phys. Lett.* **1997**, 266, 397.
- [10] R. Shah, M. C. Payne, M.-H. Lee, J. D. Gale, *Science* **1996**, 271, 1395.
- [11] E. Nusterer, P. E. Blöchl, K. Schwarz, *Angew. Chem.* **1996**, 108, 187; *Angew. Chem. Int. Ed. Engl.* **1996**, 35, 175; E. Nusterer, P. E. Blöchl, K. Schwarz, *Chem. Phys. Lett.* **1996**, 253, 448; K. Schwarz, E. Nusterer, P. E. Blöchl, *Int. J. Quant. Chem.* **1997**, 61, 369.
- [12] F. Wakabayashi, M. Kashitani, T. Fujino, J. N. Kondo, K. Domen, C. Hirose, *Stud. Surf. Sci. Catal.* **1996**, 105, 1739.
- [13] J. Bandiera, C. Naccache, *Appl. Catal.* **1991**, 69, 139.
- [14] Y. Ono, T. Mori, *J. Chem. Soc. Faraday Trans.* **1981**, 77, 2209.
- [15] T. R. Forester, R. F. Howe, *J. Am. Chem. Soc.* **1987**, 109, 5076.
- [16] “Transition State Modeling for Catalysis”: E. Sandré, M. C. Payne, I. Štich, J. D. Gale, *ACS Symp. Ser.* **1999**, 721, 346.
- [17] See, for instance, “Algorithms for Chemical Computations”: C. H. Bennett, *ACS Symp. Ser.* **1977**, 46, 63.
- [18] C. Dellago, P. G. Bolhuis, D. Chandler, *J. Chem. Phys.* **1998**, 108, 9236; *J. Chem. Phys.* **1999**, 110, 6617; C. Dellago, P. G. Bolhuis, D. Chandler, *Faraday Discuss.* **1998**, 110, 421.
- [19] E. A. Carter, G. Ciccotti, J. T. Hynes, *Chem. Phys. Lett.* **1989**, 156, 472.
- [20] “Monte Carlo and Molecular Dynamics of Condensed Matter Systems”: G. Ciccotti, M. Ferrario, in *Proceedings of Euroconference on Computer Simulation in Condensed Matter Physics and Chemistry* (Eds.: K. Binder, G. Ciccotti), SIF, Como, **1995**.
- [21] M. Sprik, G. Ciccotti *J. Chem. Phys.* **1998**, 109, 7737.
- [22] Ab initio MD simulations for ZSM-5 on a timescale of the order of 1 ps have already been performed.^[7,8] Simulations for the timescales relevant for the present simulation should be possible in due course.
- [23] P. A. Vaughan, *Acta Crystallogr.* **1966**, 21, 983.
- [24] M. C. Payne, M. P. Teter, D. C. Alan, T. A. Arias, J. D. Joannopoulos, *Rev. Mod. Phys.* **1992**, 64, 1045.
- [25] J. P. Perdew, J. A. Chevary, S. H. Vosko, K. A. Jackson, M. R. Pederson, D. J. Singh, C. Fiolhais, *Phys. Rev. B* **1992**, 46, 6671.
- [26] See, for instance, M. Boero, M. Parrinello, K. Terakura, *J. Am. Chem. Soc.* **1998**, 120, 2746.
- [27] A computer graphics animation of the simulation can be downloaded from : <http://kf-lin.elf.stuba.sk/ccms/index.html>.
- [28] S. T. Pantelides, *Phys. Rev. Lett.* **1986**, 57, 1505.

Received: December 11, 2000 [F2922]